

# Synthesis and Tribological Characterization of Cast AA1100-B<sub>4</sub>C Composites

Chennakesava R Alavala

Professor, JNT University, Hyderabad – 500 085, Telangana, India

**Abstract:** In the present work, the AA1100-B<sub>4</sub>C metal matrix composites were manufactured at 10% and 30% volume fractions of B<sub>4</sub>C. The composites were wear tested at different levels of normal load, sliding speed and sliding distances. The microstructure of worn surfaces pertaining to AA1100 alloy/ B<sub>4</sub>C composite reveals the detachment of B<sub>4</sub>C particles from the matrix.

**Keywords:** Metal matrix composite, AA1100 alloy, boron carbide, wear, sliding distance, normal load, sliding speed

## 1. Introduction

Metal Matrix Composites (MMCs) are being increasingly used in aerospace and automobile industries owing to their enhanced mechanical and tribological properties. Achievement of these properties depends primarily on the selection of reinforcement, its method of production and chemical compatibility with the matrix [1-13]. There are different types of reinforcement such as whiskers, particle, fiber and filament. Mainly particle reinforcement is preferred over the other types of reinforcement for synthesizing the metal matrix composite. The tribological behavior can be evaluated in terms of wear characteristics. The wear characteristics of these alloys depend upon the material morphology such as composition, size, shape and distribution of reinforcements and service conditions such as load, contact surface, contact time and sliding speed [14-22]. The effect of process parameters and the addition of reinforcement on the dry sliding wear of the composites were investigated vastly and explained that incorporation of hard secondary constituent in the matrix significantly improves the wear resistance.

The present work is on the evaluation of wear characteristics and consequences of cast AA1100/boron carbide composites. The design of experiments was based on Taguchi techniques [23, 24].

## 2. Materials Methods

The matrix material was AA1100 alloy. The reinforcement material was boron carbide (B<sub>4</sub>C) nanoparticles of average size 100nm. AA1100 alloy/ B<sub>4</sub>C composites were fabricated by the stir casting process and low pressure casting technique with argon gas at 3.0 bar. The composite samples were given H-18 solution treatment. The heat-treated samples were machined to get cylindrical specimens for the wear tests.

**Table 1:** Control parameters and levels

Factor	Symbol	Level-1	Level-2	Level-3
Reinforcement, Vol.%	A	10	20	30
Load, N	B	10	20	30
Speed, m/s	C	1	2	3
Sliding distance, m	D	500	1000	1500

The design of experiments was carried out as per Taguchi techniques. The levels chosen for the controllable process parameters are summarized in table 1. Each of the process

parameters was deliberated at three levels. The orthogonal array, L9 was preferred to carry out experiments as given in table 2. A pin on disc type friction and wear monitor (ASTM G99) was employed to evaluate the friction and wear behavior of AA1100 alloy/B<sub>4</sub>C composites against hardened ground steel (En32) disc. Wear test pins of 10 mm diameter and 25 mm length were prepared. The pin was mounted on a stiff lever, designed as a frictionless force transducer. The friction coefficient was determined during the test by measuring the deflection of the elastic arm. Wear coefficients for the pin and disk materials were calculated from the volume of material lost during the test. Wear tests include the measurement of:

- Weight loss using electronic weighing balance with accuracy up to 0.1 mg,
- Temperature of pin using thermocouple, and
- Friction force with data acquisition system

**Table 2:** Orthogonal array (L9) and control parameters

Treat No.	A	B	C	D
1	1	1	1	1
2	1	2	2	2
3	1	3	3	3
4	2	1	2	3
5	2	2	3	1
6	2	3	1	2
7	3	1	3	2
8	3	2	1	3
9	3	3	2	1

An investigation has been carried out to study the effects of sliding speed, contact time, normal pressure, and vol.% of B<sub>4</sub>C on the wear characteristics. Scanning electron microscopy analysis was also carried out to find consequence of wear test AA1100/B<sub>4</sub>C composite specimens.

Pukanszky et al. [25] presented an empirical relationship as given below:

$$\sigma_c = \left[ \sigma_m \left( \frac{1-v_p}{1+2.5v_p} \right) \right] e^{Bv_p} \quad (1)$$

where B is an empirical constant, which depends on the surface area of particles, particle density and interfacial bonding energy. The value of B varies between from 3.49 to 3.87.

Considering adhesion, formation of precipitates, particle size, agglomeration, voids/porosity, obstacles to the disloca-

tion, and the interfacial reaction of the particle/matrix, the formula for the strength of composite is stated below:

$$\sigma_c = \left[ \sigma_m \left\{ \frac{1 - (v_p - v_v)^{2/3}}{1 - 1.5(v_p - v_v)} \right\} \right] e^{m_p(v_p - v_v)} + k d_p^{-1/2} \quad (2)$$

$$k = E_m m_m / E_p m_p$$

where,  $v_v$  and  $v_p$  are the volume fractions of voids/porosity and nanoparticles in the composite respectively,  $m_p$  and  $m_m$  are the poisson's ratios of the nanoparticles and matrix respectively,  $d_p$  is the mean nanoparticle size (diameter) and  $E_m$  and  $E_p$  are elastic moduli of the matrix and the particle respectively. Elastic modulus (Young's modulus) is a measure of the stiffness of a material and is a quantity used to characterize materials. Elastic modulus is the same in all orientations for isotropic materials. Anisotropy can be seen in many composites.

The upper-bound equation is given by

$$\frac{E_c}{E_m} = \left( \frac{1 - v_v^{2/3}}{1 - v_v^{2/3} + v_v} \right) + \frac{1 + (\delta - 1)v_p^{2/3}}{1 + (\delta - 1)(v_p^{2/3} - v_p)} \quad (3)$$

The lower-bound equation is given by

$$\frac{E_c}{E_m} = 1 + \frac{v_p - v_v}{\delta / (\delta - 1) - (v_p + v_v)^{1/3}} \quad (4)$$

where,  $\delta = E_p / E_m$ .

The microhardness was measured in terms of Knoop hardness number. The Knoop indenter is a diamond ground to pyramidal form that produces a diamond shaped indentation having approximate ratio between long and short diagonals of 7:1. The depth of indentation is about 1/30 of its length. When measuring the Knoop hardness, only the longest diagonal of the indentation was measured and this was used in the formula mentioned in Eq. (5) with the load used to calculate KHN.

The Knoop hardness number KHN is the ratio of the load applied to the indenter,  $P$  (kgf) to the unrecovered projected area:

$$KHN = \frac{P}{CL^2} \quad (5)$$

where,

$P$  = applied load in kgf

$L$  = measured length of long diagonal of indentation in mm

$C = 0.07028$  = Constant of indenter relating projected area of the indentation to the square of the length of the long diagonal.

### 3. Results and Discussion

The mechanical properties of AA1100/B<sub>4</sub>C composites are shown in figure 1. The tensile strength was increased with volume fraction of B<sub>4</sub>C. The strength values obtained from criterion proposed by Pukanszky et al [23] are lower than the experimental values of the composites. The effect of particle size and voids/porosity were not considered in this criterion. The present criterion considers adhesion, formation of precipitates, particle size, agglomeration, voids/porosity, obstacles to the dislocation, and the interfacial reaction of the particle/matrix. The experimental strength values are in between the values obtained from the present criterion and Pukanszky et al criterion. The stiffness (figure 1b) and hardness (figure 1c) of the composites were also increased with increases of B<sub>4</sub>C content in AA1100 alloy matrix.

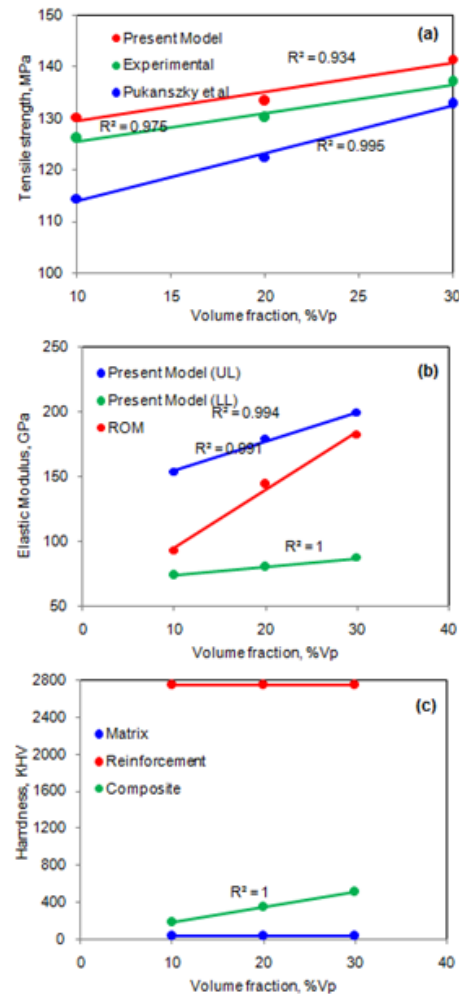


**Figure 1:** Mechanical Properties of AA1100/B<sub>4</sub>C composites.

**Table 3:** ANOVA summary of the wear rate

Source	Sum 1	Sum 2	Sum 3	SS	v	V	F	P
A	23.12	20.98	17.42	5.52	1	5.52	1.94E+14	56.81
B	18.82	20.57	22.13	1.82	1	1.82	6.43E+13	18.79
C	21.28	21.12	19.12	0.96	1	0.96	3.40E+13	9.93
D	19.48	131.60	61.52	1.40	1	1.40	4.96E+13	14.48
e				0.00	4	0.00	1.00E+00	0
T	82.70	194.27	120.19	9.72	8			100

**Note:** SS is the sum of square, v is the degrees of freedom, V is the variance, F is the Fisher's ratio, P is the percentage of contribution and T is the sum squares due to total variation.

#### 3.1 Effect of volume fraction, Normal Load, Sliding Speed, Sliding distance on Wear Rate

For the analysis of variance (ANOVA), all parameters qualify Fisher's test at 90% confidence level. In table 3, the percent contribution indicates that the parameter A, vol.% of B<sub>4</sub>C contributes nearly half (56.81%) of variation in the wear rate. The normal load (B) adds 18.79% of variation in the wear rate. The speed (C) tends 9.93% of variation in the wear rate. The sliding distance (D) presents 14.48% of variation in the wear rate.

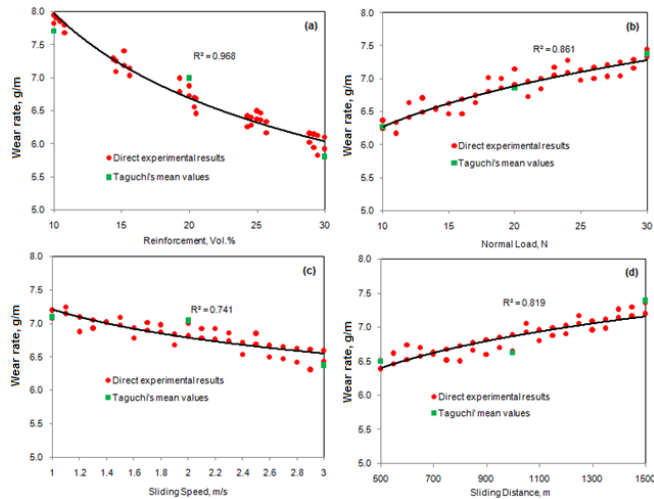


**Figure 2:** Influence of process parameters on wear rate

The wear rate was decreased with increase in volume fraction of B<sub>4</sub>C in AA1100 alloy matrix (figure 2a). This is owing to high hardness of B<sub>4</sub>C as compared to soft AA1100 alloy matrix. Composites produced by low volume fraction of B<sub>4</sub>C wear out faster than those produced by high volume fraction of B<sub>4</sub>C. The wear rate was increased with load regardless of composition of the composites as shown in figure 2b. Akbulut et al. [19] carried out wear test on Al-SiC varying the volume fraction range from 5-20 vol%. The results showed that wear rate increases with increase in load but decreases with increase in volume fraction. The wear rate was decreased with increase of sliding speed (figure 2c). Increasing the sliding speed made it increasingly difficult for surface damage by plastic deformation. From figure 2d it is observed that the wear rate was increased with the sliding distance. During sliding, as the sliding distance increases the time of contact between the surfaces were also increased. Hence, more volume loss will be there. Iwai et al. [20] studied the wear properties of SiC whisker reinforced 2024 aluminum alloy with volume fraction ranging from 0-16% produced by powder metallurgy process. The wear rate increased with increase in sliding distance and gradually severe to mild wear transition occurred. The mathematical relations between wear and vol.% of reinforcement, normal load, speed and sliding distance are given by

$$W_{rp} = 14.34 \times v_f^{-0.25} \quad (6)$$

$$W_{rf} = 4.69 \times F^{0.135} \quad (7)$$

$$W_{rn} = 7.21 \times N^{-0.08} \quad (8)$$

$$W_{rd} = 3.40 \times d^{0.102} \quad (9)$$

where,

$W_{rp}$  is the wear rate due to vol.% of reinforcement ( $v_f$ ), g/m

$W_{rf}$  is the wear rate due to normal load ( $F$ ), g/m

$W_{rn}$  is the wear rate due to speed ( $N$ ), g/m

$W_{rd}$  is the wear rate sliding distance ( $d$ ), g/m.

The R-squared values, which are attributable to vol.% reinforcement, normal load, sliding speed and sliding distance, are 0.968, 0.861, 0.741 and 0.819, respectively. This trend is similar to the percent contributions of process parameters obtained from Taguchi techniques. Therefore, R-squared values represent not only the fitness of curve but also the strength of process variables.

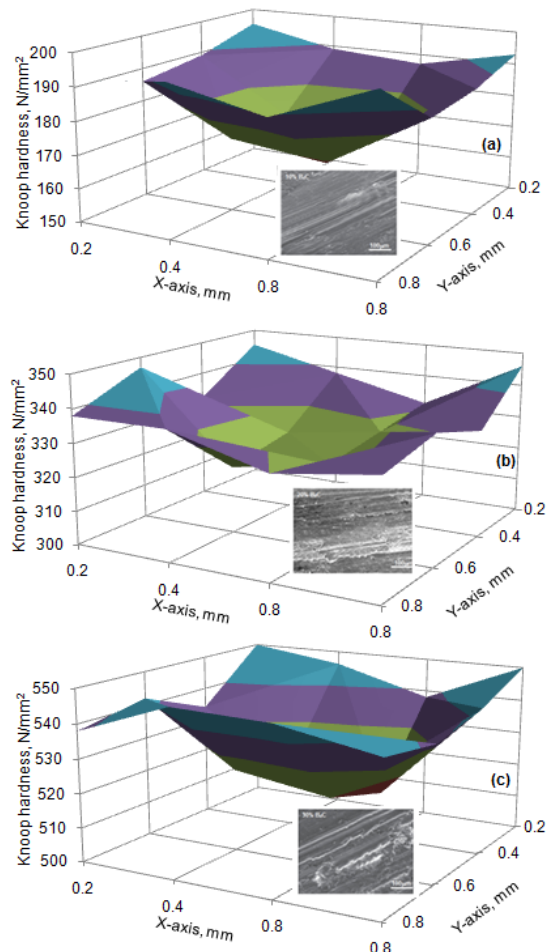


**Figure 3:** Hardness of AA1100/B<sub>4</sub>C composites after wear test: (a) 10 vol.% B<sub>4</sub>C (b) 20 vol.% B<sub>4</sub>C and (c) 30 vol.% B<sub>4</sub>C.

### 3.2 Consequence of Wear in AA1100/B<sub>4</sub>C Composites

The amount of metal loss depends upon the strength of the variables. It is necessary to distinguish the consequence of wear in AA1100/B<sub>4</sub>C composites. The purpose of post-wear evaluation is to focus the changes that are brought in the worn specimens in terms of mechanical properties, micro-structure, and worn-surface pattern. The change in hardness of the worn specimens is shown in figure 3. It can be seen that the hardness values increase after wear test. The micro-structures of worn specimens are also revealed in figure 3. The increase in hardness in the worn specimens may be attributed to the work (strain) hardening mainly due to influence of vol.% B<sub>4</sub>C. When the reinforcement increased from 10 to 30 vol.% the scratches were also increased due to detached B<sub>4</sub>C nanoparticles on the surface.

## 4. Conclusion

The investigation on the wear behavior of the composites as the function of vol.% of reinforcement, load, speed and sliding distance using Taguchi's design of experiments was carried out successfully. The following are drawn from the present work as follows:

- 1) The wear loss decreases with increase of vol.% B<sub>4</sub>C in AA1100 alloy matrix.
- 2) The wear loss increases with increase in normal load and sliding distance.

3) The wear loss decreases with increasing speed.

## References

- [1] A. C. Reddy, Fracture behavior of brittle matrix and alumina trihydrate particulate composites, *Indian Journal of Engineering & Materials Sciences*, 9, pp.365-368, 2002.
- [2] A. C. Reddy, S. Sundararajan, Influences of ageing, inclusions and voids on the ductile fracture mechanism of commercial Al-alloys, *Journal of Bulletin of Material Sciences*, 28, pp. 75-79, 2005.
- [3] A. C. Reddy, Tensile fracture behavior of 7072/SiCp metal matrix composites fabricated by gravity die casting process, *Materials Technology: Advanced Performance Materials*, 26, pp. 257-262, 2011.
- [4] A. C. Reddy, Influence of strain rate and temperature on superplastic behavior of sinter forged Al6061/SiC metal matrix composites, *International Journal of Engineering Research & Technology*, 4, pp.189-198, 2011.
- [5] A. C. Reddy, Evaluation of mechanical behavior of Al-alloy/SiC metal matrix composites with respect to their constituents using Taguchi techniques, *i-manager's Journal of Mechanical Engineering*, 1, pp.31-41, 2011.
- [6] A. C. Reddy and Essa Zitoun, Tensile properties and fracture behavior of 6061/Al<sub>2</sub>O<sub>3</sub> metal matrix composites fabricated by low pressure die casting process, *International Journal of Materials Sciences*, 6, pp.147-157, 2011.
- [7] A. C. Reddy, Strengthening mechanisms and fracture behavior of 7072Al/Al<sub>2</sub>O<sub>3</sub> metal matrix composites, *International Journal of Engineering Science and Technology*, 3, pp.6090-6100, 2011.
- [8] A. C. Reddy, Evaluation of mechanical behavior of Al-alloy/Al<sub>2</sub>O<sub>3</sub> metal matrix composites with respect to their constituents using Taguchi, *International Journal of Emerging Technologies and Applications in Engineering Technology and Sciences*, 4, pp. 26-30, 2011.
- [9] A. C. Reddy and Essa Zitoun, Matrix al-alloys for alumina particle reinforced metal matrix composites, *Indian Foundry Journal*, 55, pp.12-16, 2009.
- [10] A. C. Reddy, Mechanical properties and fracture behavior of 6061/SiCp Metal Matrix Composites Fabricated by Low Pressure Die Casting Process, *Journal of Manufacturing Technology Research*, 1, pp.273-286, 2009.
- [11] A. C. Reddy and B. Kotiveerachari, Effect of aging condition on structure and the properties of Al-alloy / SiC composite, *International Journal of Engineering and Technology*, 2, pp.462-465, 2010.
- [12] A. C. Reddy, Tensile properties and fracture behavior of 6063/SiCP metal matrix composites fabricated by investment casting process, *International Journal of Mechanical Engineering and Materials Sciences*, 3, pp.73-78, 2010.
- [13] A. C. Reddy and Essa Zitoun, Tensile behavior of 6063/Al<sub>2</sub>O<sub>3</sub> particulate metal matrix composites fabricated by investment casting process, *International Journal of Applied Engineering Research*, 1, pp.542-552, 2010.
- [14] A. C. Reddy, S. Madahava Reddy, Evaluation of dry sliding wear characteristics and consequences of cast Al-Si-Mg-Fe alloys, *ICFAI Journal of Mechanical Engineering*, 3, pp.1-13, 2010.
- [15] A. C. Reddy, M. Vidya Sagar, Two-dimensional theoretical modeling of anisotropic wear in carbon/epoxy FRP composites: comparison with experimental data, *International Journal of Theoretical and Applied Mechanics*, 6, pp. 47-57, 2010.
- [16] A. C. Reddy and B. Kotiveerachari, Influence of microstructural changes caused by ageing on wear behaviour of Al6061/SiC composites, *Journal of Metallurgy & Materials Science*, 53, pp. 31-39, 2011.
- [17] Sudarshan, M. Surappa, Dry sliding wear of fly ash particle reinforced A356 Al composites, *Wear*, 265, pp. 349-360, 2008.
- [18] H. Ahlatci, E. Candan, H. Cimenoglu, Abrasive Wear Behavior and Mechanical Properties of Al-Si/SiC Composites *Wear*, 257, pp. 625-632, 2004.
- [19] H. Akbulut, M. Durman, F. Yilmaz, Dry Wear and Friction Properties of Al<sub>2</sub>O<sub>3</sub> Short Fiber Reinforced Al-Si (LM 13) Alloy Metal Matrix Composites, *Wear*, 215, pp. 170-179, 1998.
- [20] Y. Iwai, H. Yoneda, T. Honda, Sliding Wear Behavior of Sic whisker-reinforced Aluminum Composite, *Wear* 181-183, pp. 594-602, 1995.
- [21] L. Ceschini, C. Bosi, A. Casagrande, G. L. Garagnani, Effect of Thermal Treatment and Recycling on the Tribological Behaviour of an AlSiMg-SiCp Composite, *Wear*, 251, pp. 1377-1385, 2001.
- [22] J. K. M. Kwok, S. C. Lim, High-speed Tribological Properties of some Al/SiCp Composites: I. Frictional and Wear-rate Characteristics, *Composites Science and Technology* 59, pp. 55-63, 1999.
- [23] A. C. Reddy, V.M. Shamraj, Reduction of cracks in the cylinder liners choosing right process variables by Taguchi method, *Foundry Magazine*, 10, pp. 47-50, 1998.
- [24] A. C. Reddy, V.S.R. Murti, S. Sundararajan, Control factor design of investment shell mould from coal flyash by Taguchi method, *Indian Foundry Journal*, 45, pp. 93-98, 1999.
- [25] B. Punkanszky, B. Turcsanyi, F. Tudos, Effect of interfacial interaction on the tensile yield stress of polymer composites, In: H. Ishida, editor, *Interfaces in polymer, ceramic and metal matrix composites*, Amsterdam: Elsevier, pp.467-77, 1998.